Journal of Renewable and Sustainable Energy

Shape effect of thickness of the NREL S815 profile on the performance of the H-rotor Darrieus turbine

Cite as: J. Renewable Sustainable Energy **13**, 013301 (2021); https://doi.org/10.1063/5.0015083
Submitted: 27 May 2020 . Accepted: 07 December 2020 . Published Online: 29 January 2021

Rogelio Martinez, G. Urquiza, Laura Castro, J. C. García, Alfredo Rodríguez, Oscar Tenango Pirin, J. O. Dávalos, and Uzziel Caldiño Herrera

Journal of Renewable and Sustainable Energy | ARTICLE | scitation.org/journal/rse

Shape effect of thickness of the NREL S815 profile on the performance of the H-rotor Darrieus turbine

Cite as: J. Renewable Sustainable Energy **13**, 013301 (2021); doi: 10.1063/5.0015083
Submitted: 27 May 2020 · Accepted: 7 December 2020 ·
Published Online: 29 January 2021

Rogelio Martinez,[1] G. Urquiza,[1] Laura Castro,[1] J. C. García,[1,a)] Alfredo Rodríguez,[1] Oscar Tenango Pirin,[2] J. O. Dávalos,[2] and Uzziel Caldiño Herrera[2]

AFFILIATIONS

[1]Centro de Investigación en Ingeniería y Ciencias Aplicadas, Universidad Autónoma del Estado de Morelos, Cuernavaca, Morelos, Mexico
[2]Departamento de Ingeniería Industrial y Manufactura, Universidad Autónoma de Ciudad Juárez, Cd. Juárez, Chihuahua, Mexico

[a)]Author to whom correspondence should be addressed: jcgarcia@uaem.mx

ABSTRACT

With the aim of improving the performance of vertical axis wind turbines, in this article, the flow field and aerodynamic performance of an H-rotor Darrieus turbine are computed using computational fluid dynamics. Specifically, the power coefficient (Cp) of different airfoil profile thicknesses was evaluated as a function of tip-speed ratios (TSRs) and wind speed. Four different thicknesses of the NREL S815 airfoil were evaluated, and the TSR was varied from 0.6 to 2.25 using wind speeds of 6 and 8 m/s. As a result, the power coefficient (Cp) was calculated for each airfoil and the different tip-speed ratios. It was found that for each airfoil profile, the Cp increases when the airfoil thickness and the TSR rise, until reaching a maximum, then the Cp decreases in spite of larger thickness or TSRs. After comparing the performance of each airfoil profile, the Cp is improved 14.96% for 19.2% thicker airfoils, using a TSR of 1.725 and a wind speed of 8 m/s.

I. INTRODUCTION

In the last few years, the use of renewable energy sources has been increasing to stop or diminish air pollution produced by burning fossil fuels and to be ready for the eventual depletion of conventional fossil energy sources. Among the available options of renewable energy sources is wind energy, one of the most promising alternatives because of its high energy capacity and zero CO_2 emissions to the environment.[1] To exploit wind energy, eolic turbines are employed, which are classified into two main groups: horizontal axis wind turbines (HAWTs) and vertical axis wind turbines (VAWTs). HAWTs are used mainly to extract wind energy at large scales.[2] However, recent studies have focused on VAWT turbines due to their lower installation costs because they are mainly installed close to the ground.[3–5]

Among the different VAWT turbines available, H-Darrieus turbines are those that present the highest capacity for small-scale electricity generation,[6] have the ability to operate in urban environments which present low-speed wind conditions, changing direction, and high turbulence.[7–9] Also, they have notable advantages over HAWTs, such as their ability to work with low noise levels, their low cost moving parts, and their low-cost maintenance because they do not need a yaw control system to actively orient to the direction of the wind.[7,10] However, despite the advantages cited above, there are still some weaknesses to improve, such as low self-starting capability at certain azimuth angles and also increment the power coefficient for competing with the HAWTs.[11]

To improve the performance of the H-Darrieus turbine, researchers have analyzed mainly two aspects: the turbine self-starting ability and the variables that affect its Cp. Turbine self-starting has been studied through solidity,[7,12,13] varying the number of profiles[14–16] and with the use of hybrid rotors.[17,18] The turbine Cp has been investigated by using different aerodynamic profiles since these are the main responsible for absorbing the kinetic energy contained in the wind.

Symmetric profiles have been widely evaluated for increasing Cp of the H-Darrieus rotor; however, asymmetric profiles have become increasingly popular for VAWTs on a small-scale. Researchers have shown that an asymmetric profile has a better performance compared to symmetric NACA profiles under low-intensity wind conditions.[19,20] Sengupta *et al.*[21–23] carried out several studies in which they compared the behavior of symmetric and asymmetric profiles in the application of an H-Darrieus rotor under wind conditions less than 10 m/s. They evaluated S815, NACA 0018, and EN005 profiles under wind velocities of 6 and 8 m/s. They concluded that the asymmetric S815 profile provided the best performance achieving a Cp of 0.19, improving at the same time the self-starting capacity compared to the NACA 0018 profile. Sun *et al.*[20] evaluated six differents profiles (NACA 0018, NACA 4425, NACA 1425, S1046, Du 06-W-200, and EN0005) and they concluded that the S1046 profile had a better performance than the NACA0018 profile, considering its self-starting capacity and its Cp, which was 0.143; besides a better behavior of the asymmetric profiles was also demonstrated under wind speeds of less than 6 m/s compared to the symmetric ones. Other studies that increase the Cp have made modifications to the profiles such as removing a plate from its walls leaving a J-shaped profile,[24] modifying its walls with tubercles,[25] and changing the shape of its edge output.[26] This led to obtain improvements in efficiency but increased the complexity of its manufacture.

From the above research studies, it is observed that investigators have found different ways to improve the Cp of the H-Darrieus rotor such as the determination of the number of profiles that provide a better self-starting, the aspect ratio that improves performance, and various studies in which different aerodynamic profiles were evaluated. However, the definition of the geometric characteristics of the profiles is of great importance to improve the performance of the rotor without compromising the simplicity of the profiles. Therefore, the contribution of this work is the dynamic understanding of the behavior of the Cp of the turbine as a function of the thickness of an asymmetric S815 profile under different tip-speed ratios (TSRs) and for two wind speeds. The S815 profile was selected following the literature[21–23] where they presented improvements in the performance of the H-Darrieus rotor. The results show that Cp has an increment of 14.96%, for airfoils 19.2% thicker than standard S815 profile, at TSR = 1.725 and a wind speed of 8 m/s.

II. METHODOLOGY

A. Fundamental equations for wind turbines

In this paper, to systematically study the performance of wind turbines, some variables are grouped using dimensionless numbers: TSR and Cp. TSR is the relationship that exists between the rotor tangential speed (ω is the rotor angular speed and R is the rotor radius) and the free wind speed (U_∞), which is defined as

$$TSR = \frac{\omega R}{U_\infty}. \quad (1)$$

Cp quantifies the portion of power (P) absorbed by the turbine rotor from free wind speed

$$Cp = \frac{P}{\frac{1}{2}\rho A U_\infty^3}, \quad (2)$$

where A is the turbine rotor cross section and ρ is the air density.

Other groups of variables are solidity σ and blockage β, which are kept constant in this research. Solidity σ is a factor to determine the dimensions of the turbine and is computed as

$$\sigma = \frac{Nc}{2R}, \quad (3)$$

where N is the number of blades and c is the blade chord length.

The blockage is defined by

$$\beta = \frac{A}{A_D}, \quad (4)$$

where A_D is the cross section of the domain where the turbine is tested. In this research, $\sigma = 0.5172$ and $\beta = 0.1$, which remain constant through all computations.

B. CFD model

The effect of the airfoil maximum thickness on the VAWT turbine performance was computed using computational fluid dynamics (CFD). The target of this work is to obtain the Cp of the turbine using four variations of the thickness of the S815 profile under different operating conditions. Details of the CFD model are given in Secs. II B 2–II B 4.

1. Governing equations and turbulence model

To solve the flow field, CFD computations were carried out using ANSYS Fluent software in a transient state, solving the Reynolds-averaged Navier–Stokes equations (RANS) using the algorithm of Semi-Implicit Method for Pressure Linked Equations (SIMPLE) for pressure velocity coupling. The RANS equations are

$$\frac{\partial \overline{u_i}}{\partial_t} + \overline{u_j}\frac{\partial \overline{u_i}}{\partial x_j} = -\frac{\partial \overline{p}}{\partial x_i} + \nu\frac{\partial^2 \overline{u_i}}{\partial x_j \partial x_j} - \frac{\partial \tau_{ij}}{\partial x_j}, \quad (5)$$

$$\frac{\partial \overline{u_i}}{\partial x_i} = 0, \quad (6)$$

where $\overline{u}$ is the mean velocity, $\overline{p}$, is the mean presssure, t is the time, $\overline{\tau_{ij}}$ is the Reynolds stress tensor , and the subscripts i, j are unit vectors for the x, y, and z, directions.

The turbulence was solved employing the Renormalization Group (RNG)- k–ε turbulence model where transport equations for the turbulent kinetic energy k and the energy-dissipation rate ε are

$$\frac{\partial}{\partial t}(\rho k) + \frac{\partial}{\partial x_i}(\rho k u_i) = \frac{\partial}{\partial x_j}\left[a_k \mu_{eff}\frac{\partial k}{\partial x_j}\right] + G_k + G_b - \rho\varepsilon - Y_M + S_k, \quad (7)$$

$$\frac{\partial}{\partial t}(\rho \varepsilon) + \frac{\partial}{\partial x_i}(\rho \varepsilon u_i) = \frac{\partial}{\partial x_j}\left[a_\varepsilon \mu_{eff}\frac{\partial \varepsilon}{\partial x_j}\right] + C_{1\varepsilon}\frac{\varepsilon}{k}(G_k + C_{3\varepsilon}G_b) - C_{2\varepsilon\rho}\frac{\epsilon^2}{k} - R_\epsilon + S_\varepsilon, \quad (8)$$

where G_k is the generation of turbulence kinetic energy due to the mean velocity gradient, G_b is the generation of turbulence kinetic energy due to buoyancy, Y_M is the fluctuating incompressible diffusion, a_k and a_ε are the inverse effective Prandtl numbers, and S_k and S_ε are user-defined source terms.

In the case of wind turbine domains, where modeling rotating flows and calculating effective viscosity are needed, the RNG- k–ε turbulence model is adequate to solve such flow fields.[21,27–30]

2. Model geometry

The computational domain was divided into two parts, as shown in Fig. 1. One of them is a rotating domain that corresponds to the turbine rotor (airfoils and rotor shaft) and the other one is a stationary domain that stands for the external environment of the turbine. The dimensions of the domain are multiples of the rotor diameter, as

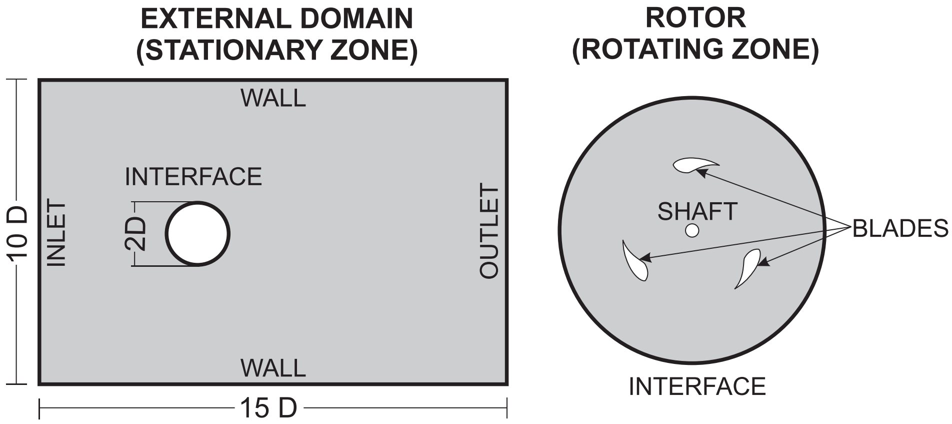

FIG. 1. Computational domain.

TABLE I. Geometry features of the rotor.

Category	Dimension
No. of blades	3
Blade height (m)	0.29
Rotor diameter (m)	0.29
Blade chord (m)	0.05

shown in Fig. 1. Taking the center of the turbine rotor, the dimensions of the rectangular domain were five diameters upstream, 10 diameters downstream, and five diameters at each side of the turbine. The turbine rotor is in a circular domain of two rotor diameters (Table I shows the H-Darrieus rotor dimensions).

Four different airfoil thicknesses of the NREL S815 profile were investigated. The S815 profile thickness was increased by 12.8%, 19.2%, and 32% at the lower wall, as shown in Fig. 2. The NREL S815 profile was used in this research because Sengupta *et al.*[21] reported a high performance of this profile in comparison with the NACA0018 and EN0005 profiles.

3. Boundary conditions

The boundary conditions used were a velocity condition at the inlet, an outflow at the exit, and an interface between the two computational domains (rotor and external domains). Regarding to rotor limits, the no-slip condition was used in the near-wall region of blades.

The performance of the wind turbine profiles was investigated at a different TSR (0.6–2.25) using two conditions of wind speeds: 6 and 8 m/s as the inlet velocity condition. To compute the aerodynamic

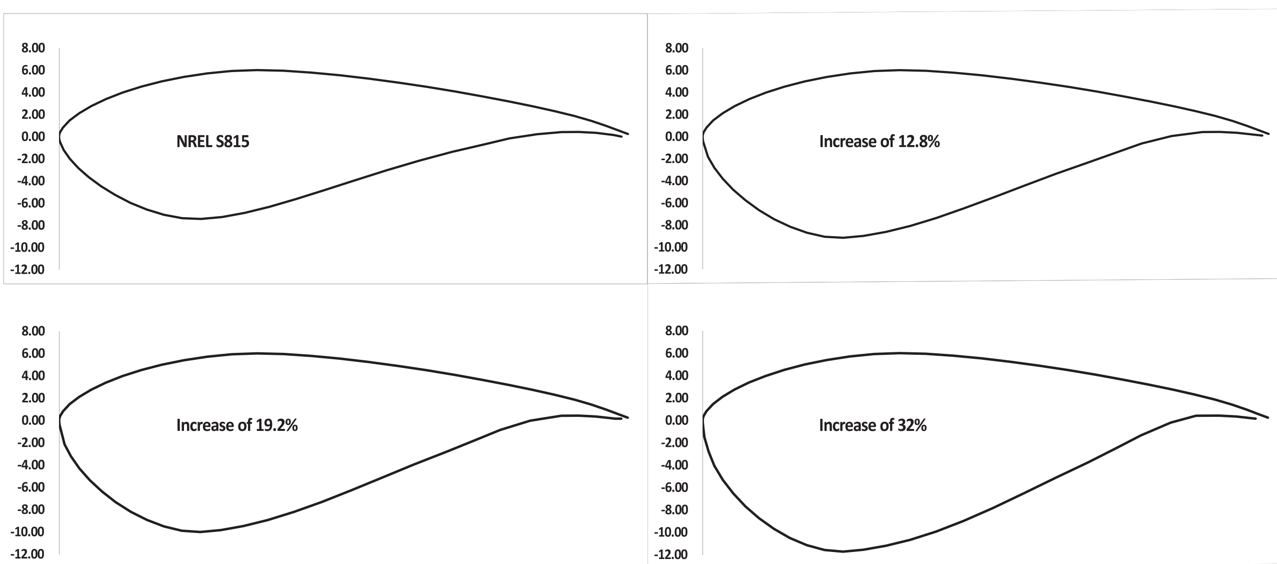

FIG. 2. Evaluated geometries.

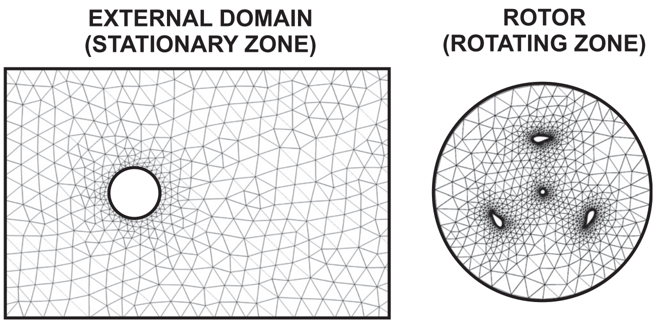

FIG. 3. External and rotor domain grids.

performance of the turbine, the torque was recorded every 1/360 parts of the turbine rotation during 15 turbine rotations.

4. Mesh generation

The domains were meshed using tetrahedral mesh and near the wall blades the mesh was decreased in size as shown in Fig. 3. The length of the elements near of walls was 0.35 mm. To take into account the effect of the boundary layer, the wall standard function for the RNG- k–ε turbulence model was used .

C. Independence mesh analysis and code validation

To select the appropriate number of mesh elements to satisfy the computation accuracy and cost, a mesh independence study was carried out by using five different densities of meshes. The relative error (RE) values obtained are listed in Table II where Mesh 2 has the lowest RE. However, Mesh 3 has a closer RE than Mesh 2 and in addition it has less number of elements which reduce the computational cost, so Mesh 3 was selected to perform all computations.

After performing mesh independence analysis, the model was validated through a comparison of the power between the numerical computations and experimental data reported by Sengupta *et al.*[21]

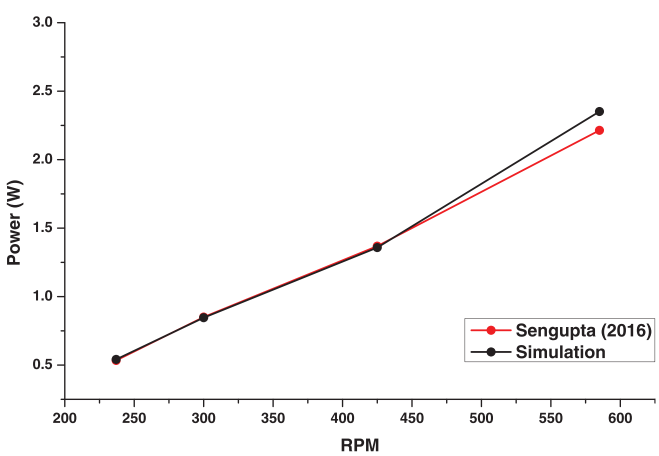

FIG. 4. Comparison of simulated numerical power and experimental data reported by Sengupta *et al.*[21]

TABLE II. Relative error calculation.

Mesh	No. of elements	Torque (N·m)	RE
Mesh 1	1 875 747	0.027 69	
Mesh 2	1 614 285	0.025 31	8.60
Mesh 3	1 321 123	0.025 30	8.63
Mesh 4	1 215 290	0.024 92	10.01
Mesh 5	1 149 064	0.021 20	23.44

(Fig. 4), taking into consideration 4% mechanical losses. The maximum difference with respect to the data experimental data is 6.5%.

III. RESULTS AND DISCUSSION

The aerodynamic operation of a Darrieus turbine is influenced by multiple parameters, within which, the drag and lift forces caused by the geometry of the aerodynamic profiles are of great importance; the relationship of these forces generates a dynamic torque which, together with the rotation of the turbine, generates power. Cp is the relationship between the power generated by the turbine and the power contained in the air. This article studies the Cp of the turbine when using different thicknesses of the S815 profile.

A. Power coefficient (Cp)

The Cp of an H-Darrieus turbine was investigated as a function of the aerodynamic performance of its blades (S815 profile). Therefore, CFD computations were carried out to determine the wind turbine Cp using four different thicknesses of the S815 airfoil under wind speeds of 6 m/s and 8 m/s. As a result, dynamic torque evolution per revolution was obtained through the monitors placed in the rotating shaft. The monitors collected the sum of instantaneous torque provided by the three blades in every grade of rotation. The wind turbine Cp was calculated using the average torque values from each of the simulations using Eq. (2).

Figure 5 shows the power coefficients for all airfoil thicknesses at different winds velocities [6 m/s (a) and 8 m/s (b)] and tip-speed ratios. This figure shows that the power coefficient increases for all airfoils by increasing the speed ratio until it reaches the 1.7 tip-speed ratio. Then it starts to decrease; this action develops for both wind speeds.

Similarly, when observing the maximum points of the Cp obtained by each of the airfoils, a clear influence of the thickness airfoil on the Cp is shown, developing a behavior similar to that of the tip-speed ratio since the Cp increases proportionately to the thickness profile, until it reaches a maximum point for airfoils 19.2% thicker. The highest values of Cp were obtained by using the profile whose thickness was increased by 19.2% with a tip speed ratio of 1.7125, 0.26 with an incident wind speed of 6 m/s Fig. 5(a) and 0.28 with an incident wind speed of 8 m/s Fig. 5(b).

Figure 6 illustrates the instantaneous polar distribution of the turbine Cp throughout a revolution with different S815 airfoil thicknesses at the two wind speeds using the speed ratio where the highest Cp values are achieved (1.7125). The polar graphs have three peaks which represent the maximum points reached by the turbine in each revolution, with the number of peaks being equal to the number of airfoils of the turbine as explained by Lain and Osorio in their study,[31] The main

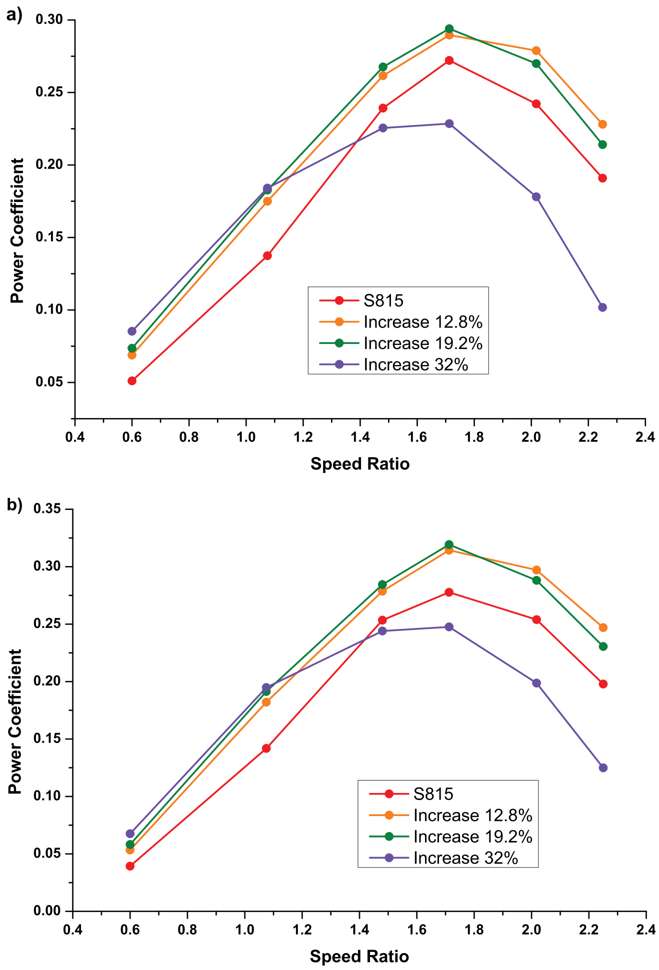

FIG. 5. TSR curves vs Cp of the evaluated profiles: (a) 6 m/s and (b) 8 m/s.

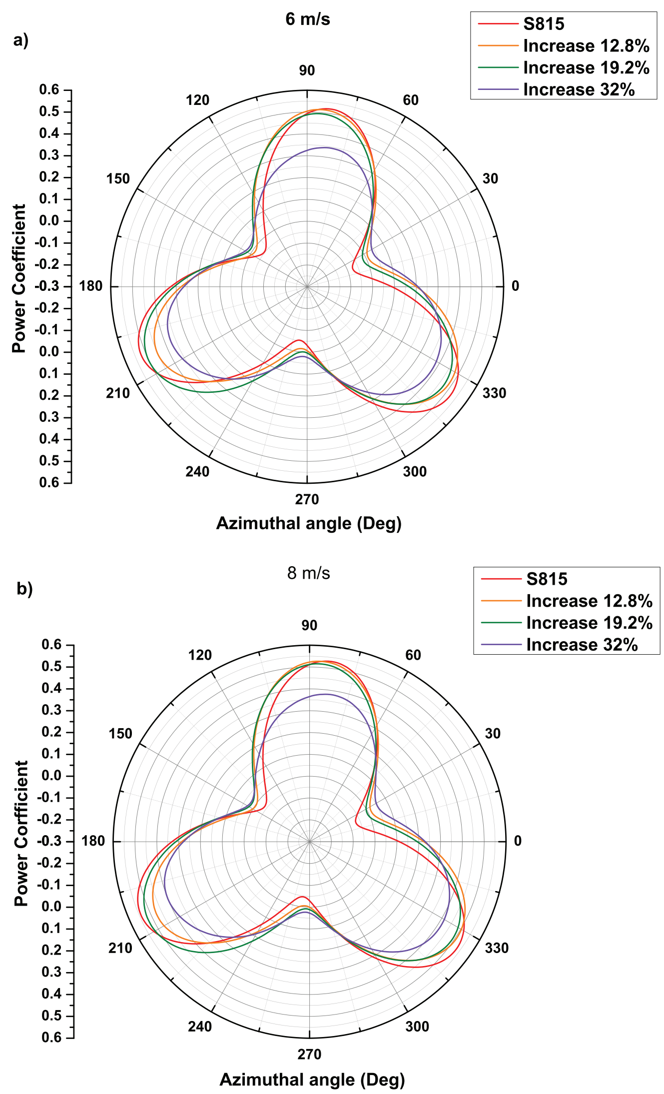

FIG. 6. Instantaneous Cp polar plots: (a) 6 m/s and (b) 8 m/s.

change in the maximum peaks is observed with the use of airfoil profiles 32% thicker, since lower values are obtained in both wind speeds compared to the other profiles. On the other hand, at minimum points, the S815 airfoil achieves the lowest values at both wind speeds.

Considering that the Cp of the turbine corresponds to the average of the maximum and minimum points of the cycles within the rotation, the values of Cp obtained by the profile 19.2% thicker were the highest of all the profiles evaluated, exceeding 8% to the S815 airfoil at wind speeds of 6 m/s and 14.96% at 8 m/s.

B. Static pressure contour

As a result of the post-processing of the simulations, the pressure contours were obtained to understand the behavior of the wind flow in contact with the turbine profiles and determine the reason for the power results obtained by modifying the thickness of the S815 airfoil. To simplify this analysis, only the S815 airfoil and airfoil 19.2% thicker were considered, since it showed the highest results in both wind speeds.

Figures 7 and 8 depict turbine static pressure contours using the S815 airfoil and the airfoil with a thickness increase of 19.2% with wind speeds of 6 and 8 m/s, respectively. Figures 7(a) and 8(a) show the favorable angular position and Figs. 7(b) and 8(b) show the unfavorable position of blades.

Comparing the original airfoil and the airfoil 19.2% thicker in Fig. 7(a), it can be seen that the airfoil with increased thickness has a higher pressure compared to the original, this increase in pressure occurs mainly when the airfoil position is perpendicular to the wind flow, which causes a greater torsional force.

Similarly, Fig. 7(b) shows that, at the angular position of 320°, the modified airfoil has higher pressure at its lower surface and higher suction in the upper wall of the airfoil compared with the S815. Meanwhile, in Fig. 8(b), the same behavior can be appreciated, but it is

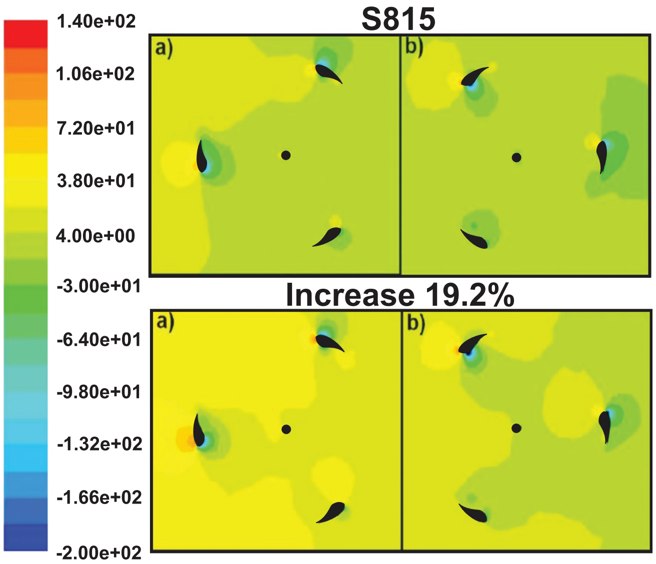

FIG. 7. Static pressure (Pa) contour plot at 6 m/s, (a) favorable angular blades position and (b) unfavorable angular blades position.

augmented because of the increase in wind speed. This is the reason why Cp rises when the maximum thickness is modified up to 19.2%.

IV. CONCLUSIONS

In the current work, a transient CFD model is used to analyze the effect of the maximum thickness of the S815 profiles on the power coefficient of a three-bladed H-Darrieus turbine. Four different thicknesses of the NREL S815 airfoil under two wind speeds and six TSRs were investigated. The conclusions of this work are summarized as follows:

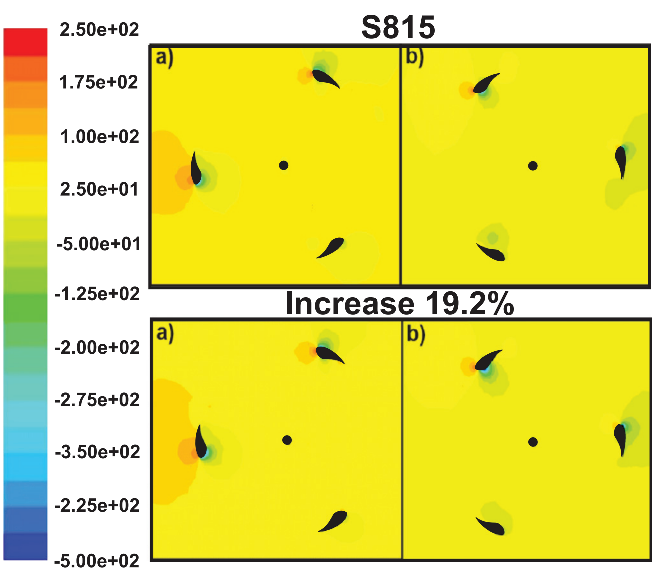

FIG. 8. Static pressure (Pa) contour plot at 8 m/s, (a) favorable angular blades position and (b) unfavorable angular blades position.

- The average power coefficient of the H-Darrieus rotor increases with the thickness of the profile until reaching a maximum point; profile 19.2% thicker. Once this thickness is exceeded, the power coefficient decreases due to aerodynamic resistance; this behavior is maintained at both wind speeds.
- Higher power coefficients for all rotor configurations were found at a TSR of 1.7125.
- The maximum computed power coefficient was obtained for the profile 19.2% thicker for both wind speeds. The increase in power coefficients with respect to the original profiles was 8% for a wind speed of 6 m/s and 14.96% for a wind speed of 8 m/s.
- The polar plots of power coefficients allow identifying the angular positions where the extraction of kinetic energy is maximum or minimum. The polar plot shows that the profiles 32% thicker can increase the power coefficients in the angular position where the rest of the profiles are low. This fact means that 32% thicker could have a self-starting faster than other profiles.

These results are a database that shows the relation between profile thickness and the power coefficients taking into account the TSR and wind speeds. This database could be used as initial data for an optimization algorithm in order to find a global maximum.

In this research, we use TSR and Cp as a key dimensionless group, which lets us to transfer the results of the geometrical model profiles in this paper to a prototype with another size; however, our computations are restricted to the boundary conditions imposed on the computational model.

AUTHORS' CONTRIBUTIONS

All authors contributed equally to this work.

ACKNOWLEDGMENTS

The main author would like to thank the Science and Technology National Council (CONACyT) for the economic support for his graduate studies (Grant No. 745525) which led to the development of this work.

DATA AVAILABILITY

The data that support the findings of this study are available within the article.

REFERENCES

[1] A. A. Khan, Z. Mehmood, and A. Shahzad, "Evaluation of wind energy potential alongside motorways of Pakistan," Asian J. Appl. Sci. Eng. **3**(9), 7–13 (2014).

[2] R. Howell, N. Qin, J. Edwards, and N. Durrani, "Wind tunnel and numerical study of a small vertical axis wind turbine," Renewable Energy **35**(2), 412–422 (2010).

[3] L. Nguyen and M. Metzger, "Optimization of a vertical axis wind turbine for application in an urban/suburban area," J. Renew. Sustain. Energy **9**(4), 043302 (2017).

[4] Q. Wang, J. Wang, Y. Hou, R. Yuan, K. Luo, and J. Fan, "Micrositing of roof mounting wind turbine in urban environment: CFD simulations and lidar measurements," Renewable Energy **115**, 1118–1133 (2018).

[5] E. Arteaga-López, C. Angeles-Camacho, and F. Bañuelos-Ruedas, "Advanced methodology for feasibility studies on building-mounted wind turbines

installation in urban environment: Applying CFD analysis," Energy **167**, 181–188 (2019).
[6] W. Tjiu, T. Marnoto, S. Mat, M. H. Ruslan, and K. Sopian, "Darrieus vertical axis wind turbine for power generation I: Assessment of Darrieus VAWT configurations," Renewable Energy **75**, 50–67 (2015).
[7] M. A. Singh, A. Biswas, and R. D. Misra, "Investigation of self-starting and high rotor solidity on the performance of a three S1210 blade H-type Darrieus rotor," Renewable Energy **76**, 381–387 (2015).
[8] S. Zanforlin and S. Letizia, "Effects of upstream buildings on the performance of a synergistic roof-and-diffuser augmentation system for cross flow wind turbines," J. Wind Eng. Ind. Aerodyn. **184**, 329–341 (2019).
[9] A. Kc, J. Whale, and T. Urmee, "Urban wind conditions and small wind turbines in the built environment: A review," Renewable Energy **131**, 268–283 (2019).
[10] I. Hashem and M. H. Mohamed, "Aerodynamic performance enhancements of H-rotor Darrieus wind turbine," Energy **142**, 531–545 (2018).
[11] M. H. Mohamed, "Performance investigation of H-rotor Darrieus turbine with new airfoil shapes," Energy **47**(1), 522–530 (2012).
[12] O. Eboibi, L. Angelo, M. Danao, and R. J. Howell, "Experimental investigation of the in fluence of solidity on the performance and flow field aerodynamics of vertical axis wind turbines at low Reynolds numbers," Renewable Energy **92**, 474–483 (2016).
[13] S. B. Qamar and I. Janajreh, "A comprehensive analysis of solidity for cambered Darrieus VAWTs," Int. J. Hydrogen Energy **42**(30), 19420–19431 (2017).
[14] M. Castelli, S. De Betta, and E. Benini, "Effect of blade number on a straight-bladed vertical axis wind turbine," Int. J. Mech. Aerospace, Ind. Mechatron. Manuf. Eng. **6**(1), 305–311 (2012).
[15] Q. Li, T. Maeda, Y. Kamada, J. Murata, K. Furukawa, and M. Yamamoto, "Effect of number of blades on aerodynamic forces on a straight-bladed vertical axis wind turbine," Energy **90**, 784–795 (2015).
[16] A. Rezaeiha, H. Montazeri, and B. Blocken, "Towards optimal aerodynamic design of vertical axis wind turbines: Impact of solidity and number of blades," Energy **165**, 1129–1148 (2018).
[17] M. H. Mohamed, "Impacts of solidity and hybrid system in small wind turbines performance," Energy **57**, 495–504 (2013).
[18] X. Liang, S. Fu, B. Ou, C. Wu, C. Y. H. Chao, and K. Pi, "A computational study of the effects of the radius ratio and attachment angle on the performance of a Darrieus-Savonius combined wind turbine," Renewable Energy **113**, 329–334 (2017).
[19] A. Bianchini *et al.*, "On the influence of virtual camber effect on airfoil polars for use in simulations of Darrieus wind turbines," Energy Convers. Manage. **106**, 373–384 (2015).
[20] X. Sun, J. Zhu, A. Hanif, Z. Li, and G. Sun, "Effects of blade shape and its corresponding moment of inertia on self-starting and power extraction performance of the novel bowl-shaped floating straight-bladed vertical axis wind turbine," Sustainable Energy Technol. Assess. **38**, 100648 (2020).
[21] A. R. Sengupta, A. Biswas, and R. Gupta, "Studies of some high solidity symmetrical and unsymmetrical blade H-Darrieus rotors with respect to starting characteristics, dynamic performances and flow physics in low wind streams," Renewable Energy **93**, 536–547 (2016).
[22] A. R. Sengupta, A. Biswas, and R. Gupta, "The aerodynamics of high solidity unsymmetrical and symmetrical blade H-Darrieus rotors in low wind speed conditions," J. Renewable Sustainable Energy **9**(4), 043307 (2017).
[23] A. R. Sengupta, A. Biswas, and R. Gupta, "Comparison of low wind speed aerodynamics of unsymmetrical blade H-Darrieus rotors-blade camber and curvature signatures for performance improvement," Renewable Energy **139**, 1412–1427 (2019).
[24] M. Zamani, S. Nazari, S. A. Moshizi, and M. J. Maghrebi, "Three dimensional simulation of J-shaped Darrieus vertical axis wind turbine," Energy **116**, 1243–1255 (2016).
[25] S. Lin, Y. Lin, C. Bai, and W. Wang, "Performance analysis of vertical-axis-wind-turbine blade with modified trailing edge through computational fluid dynamics," Renewable Energy **99**, 654–662 (2016).
[26] M. Baghdadi, S. Elkoush, B. Akle, and M. Elkhoury, "Dynamic shape optimization of a vertical-axis wind turbine via blade morphing technique," Renewable Energy **154**, 239–251 (2020).
[27] H. Beri and Y. Yao, "Effect of camber airfoil on self-starting of vertical axis wind turbine," J. Environ. Sci. Technol. **4**, 302–312 (2011).
[28] L. X. Zhang, Y. B. Liang, X. H. Liu, Q. F. Jiao, and J. Guo, "Aerodynamic performance prediction of straight-bladed vertical axis wind turbine based on CFD," Adv. Mech. Eng. **5**, 905379 (2012).
[29] P. Deshpande and X. Li, "Numerical study of giromill-type wind turbines with symmetrical and non-symmetrical airfoils," Eur. Int. J. Sci. Technol. **2**(8), 195–208 (2013).
[30] Y. Chen and Y. Lian, "Numerical investigation of vortex dynamics in an H-rotor vertical axis wind turbine," Eng. Appl. Comput. Fluid Mech. **9**(1), 21–32 (2015).
[31] S. Lain and C. Osorio, "Simulation and evaluation of a straight-bladed Darrieus-type cross flow marine turbine," J. Sci. Ind. Res. J. **69**, 906–912 (2010), http://nopr.niscair.res.in/handle/123456789/10657.